Article

Location Dependence of Mass Sensitivity for Acoustic Wave Devices

Kewei Zhang [1], Yuesheng Chai [1] and Z.-Y. Cheng [2],*

[1] School of Materials Science and Engineering, Taiyuan University of Science and Technology, Taiyuan 030024, China; E-Mails: zhangk1@tigermail.auburn.edu (K.Z.); cys5912@126.com (Y.C.)

[2] Materials Research and Education Center, Auburn University, Auburn, AL 36849, USA

* Author to whom correspondence should be addressed; E-Mail: chengzh@eng.auburn.edu; Tel.: +1-334-844-3419.

Academic Editor: Vittorio M. N. Passaro

Abstract: It is introduced that the mass sensitivity (S_m) of an acoustic wave (AW) device with a concentrated mass can be simply determined using its mode shape function: the S_m is proportional to the square of its mode shape. By using the S_m of an AW device with a uniform mass, which is known for almost all AW devices, the S_m of an AW device with a concentrated mass at different locations can be determined. The method is confirmed by numerical simulation for one type of AW device and the results from two other types of AW devices.

Keywords: mass sensitivity; acoustic wave device; point mass; biosensor; microcantilever; magnetostrictive particles

1. Introduction

Acoustic wave (AW) devices have been widely studied and used as sensor platforms for the development of various sensors, including physical, biological, and chemical sensors [1–5]. Various AW devices, such as bulk and micro- or nano-AW devices with different geometries, have been developed for these purposes [1,2]. Although the geometries of AW devices can be very different, the principle of all AW devices as sensor platforms is the same [1]: the resonant frequency of an AW device changes with the influence of the environment, such as viscosity, temperature, friction force, and mass load. For the comparison and performance/fundamental study of AW devices, a mass sensitivity ($S_m = -\Delta f/\Delta m$, in

the unit of Hz/g) is introduced to characterize the capability of AW devices as sensor platforms. The S_m is defined as the shift in the resonant frequency (Δf) due to the attachment of a mass load (Δm) onto the surface of the AW device [6]. If the mass load is uniformly distributed over the entire surface of an AW device, it is obtained for most of the AW devices that [6,7]:

$$S_m^{uni} = -\frac{\Delta f}{\Delta m} \approx \frac{f_0}{2M} \ (\Delta m << M) \tag{1}$$

where M and f_0 are the mass and the resonant frequency of the AW device without a mass load. However, the mass load is usually localized (*i.e.*, the mass load is not uniformly distributed) on the surface of an AW device for most applications. Therefore, from an application point view, it is of interest to know the S_m of an AW to a concentrated mass at different locations.

It is well known that the S_m of an AW device is strongly dependent on the location of the mass load [1,8]. That is, for the same mass load attached to the surface of an AW device, the change in the resonant frequency of the AW device is dependent on where (the location) the mass load is. For example, if the mass load is at the node point of an AW device, a zero frequency change (*i.e.*, zero S_m) is expected. In other words, the change in the resonant frequency of an AW device is dependent on both the mass load and the location of this mass load. Therefore, it is critical to know the relationship between the mass sensitivity and the location of the mass load in order for anyone to use the AW device to determine/measure the mass load based on the change in the resonant frequency. Unfortunately, there are no results on how the location will affect the S_m due to the fact that there is no analytic solution.

For some classic applications, the influence of the environment on the surface of an AW device is uniform. For example, the well-known quartz microbalance is widely used in the characterization/measurement of the thickness of a thin film, where the mass load is a uniformly distributed layer over the sensor surface. In this case, the widely-used mass sensitivity is actually defined as the sensitivity with a unit of $Hz/(g/cm^2)$ for measuring surface density rather than the sensitivity with a unit of Hz/g for measuring the mass itself [1,2]. Even for these widely used AW devices, the mass sensitivity for a concentrated mass is unknown.

In recent years, AW devices have been extensively studied for the development of biological and chemical sensors due to the fact that the AW devices, as a sensor platform, exhibit an unprecedented sensitivity and can be easily miniaturized [9,10]. As demonstrated by the experimental results and indicated by the theoretical research, biosensors using AW devices as sensor platforms show many advantages, especially for the detection of bacteria and viruses, over biosensors using electrochemical and optical devices as sensor platforms [11]. When the biosensors based on AW devices are used for the detection of bacteria, the bacterial cells are bound on the sensor surface as individual particles rather than a uniform thin layer. In this case, the mass load (*i.e.*, bound bacterial cells) is localized. Therefore, the change in the resonant frequency due to a bacterial cell bound on the surface is strongly dependent on the location of the cell. To estimate the bound bacterial cells on the sensor surface by using the measured change in the resonant frequency, it is important to know the relationship between the S_m and the mass-load location. Additionally, if the location dependence of the S_m can be quantified, the AW devices can be developed to measure nanoparticles and the interaction between different nanoparticles. Knowing the location dependence of the S_m would also make it is possible to optimize/enhance the performance of the sensors based on AW devices. For example, since it is known that the S_m reaches its

maximum when the mass load is at the free end of a cantilever, a viscosity sensor was developed using a cantilever [12].

Although the location dependence of the S_m is important, it is not known for all AW devices since there is no analytic solution for the location dependence of the S_m for any AW device [1,5]. Here, a new methodology is introduced to simply determine the S_m for a concentrated mass at different locations. The methodology is first proposed based on the numerical simulation of a typical kind of AW device—freestanding magnetostrictive strips, also known as magnetostrictive particles (MSPs) [13,14]. The methodology is then used to determine the location dependence of the S_m for two other types of AW devices—cantilever and diaphragm. The results from this new methodology are compared with, and confirmed by, the results obtained for a special point on a cantilever and diaphragm using the effective mass approach with some approximations: the S_m for a concentrated mass at the free end of a cantilever and the S_m for a concentrated mass at the middle of a diaphragm.

2. Theoretical Consideration and Numerical Simulation

MSPs have been developed as a type of AW device for the development of high-performance sensors due to the fact that the MSPs, as a sensor platform, exhibit some unique advantages over other AW devices [11,13]. An MSP is a strip of a magnetostrictive material, whose length changes when subjected to a magnetic field. Sensors using MSPs as sensor platforms exhibit high performance [11–17]. For example, for the *in situ* and real-time detection of bacteria in water, a detection limit less than 10^2 cfu/ml has been obtained for the detection of different pathogenic bacteria in liquid [11].

For an MSP with a length of L, a width of W, and a thickness of H, its fundamental resonant frequency (f_0) for the longitudinal vibration is [8,18]:

$$f_0 = \frac{1}{2L}\sqrt{\frac{E}{\rho(1-\sigma)}} \quad (L >> W >> H) \tag{2}$$

where, E, ρ and σ are the Young's modulus, density, and the Poisson's ratio of the magnetostrictive material, respectively.

If a concentrated mass is attached on to the surface of an MSP, the resonant frequency cannot be obtained with an analytic solution. For numerical simulation, assume an MSP is a plane-stress dominated isotropic elastic plate so that the $E_{\text{plane-stress}} = E/(1-\sigma)$. When an MSP with a concentrated mass is excited to resonate along the x-axis (*i.e.* length direction), the kinetic energy (T) and potential energy (V) of the MSP can be expressed as:

$$T = \frac{1}{2}\int_0^L \rho \cdot A_s \cdot \left(\frac{\partial u(x,t)}{\partial t}\right)^2 dx + \frac{1}{2}\Delta m \cdot \left(\frac{\partial u(x,t)}{\partial t}\right)^2_{x=x_c} \tag{3}$$

$$V = \frac{1}{2}\int_0^L \frac{E}{1-\sigma} A_s \left(\frac{\partial u(x,t)}{\partial x}\right)^2 dx \tag{4}$$

where, t is the time; Δm is the concentrated mass load at a location x_c ($0 \leq x_c \leq L$); A_s is the cross-sectional area ($W \times H$) of the MSP; $u(x,t)$ is the displacement vector along the x-axis; the first and second terms on the right side in Equation (3) represent the kinetic energy for the MSP and the Δm. The $u(x,t)$ can be expressed as: $u(x,t) = \varphi(x) \cdot q(t)$, where $u = [u_1, u_2, ..., u_n]$, u_n is the displacement for the *n*th

order resonance. $\varphi(x) = [\varphi_1, \varphi_2, \ldots, \varphi_n]$ is the mode shape vector, where $\varphi_n(x)$ is the mode shape function of the *n*th order resonance. $q(t)$, generalized coordinately, is an $n \times n$ matrix. Therefore, the governing vibration equation is derived to determine the *n*th order resonant frequency (f_n) of an MSP with a concentrated mass load. Based on these, and using the same procedure as described by Zhang *et al.* [19], the numerical simulation can be carried out to determine the resonance frequency of an MSP with a concentrated mass load. For the numerical simulation, MATLAB software was used with the properties and dimension of the MSP listed in Table 1.

Table 1. Parameters for the MSP used in the numerical simulation.

	Symbol	**Unit**	**Value**
Young's modulus	E	GPa	10^5
Density	ρ_s	kg/m^3	7.9×10^3
Poisson's ratio	v	-	0.33
Length	L	mm	1
Width	W	mm	0.2
Thickness	H	μm	15

The properties listed in Table 1 are the same as those of Metglas^{TM} 2826 MB [20], which is widely used in the development of MSP-based sensors. Using Equations (1) and (2) with the properties and dimension listed in Table 1, it is obtained that the fundamental resonant frequency (f_0) is 2.22697 MHz and the $S_m^{uni} = 46.98$ Hz/ng.

If $\Delta m = 0$, the numerical simulation results in a f_0 of 2.22697 MHz, which is the same as what was obtained from Equation (2). This also shows the correctness of the numerical simulation approach used here.
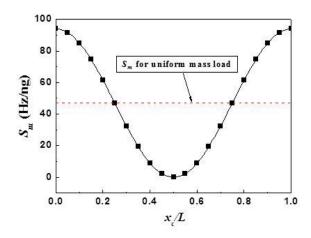

Figure 1. Simulated S_m (solid squares) for the concentrated mass load at different locationsm (x_c) for the MSP operated at the fundamnetal resonant mode. The parameters of the MSP is listed in Table 1. The numerical simulation is done for a mass load of $M^* = \Delta m/M = 10^{-5}$. The solid line is the fitting curve.

To simulate the S_m, let $\Delta m/M = 1 \times 10^{-5}$ (*i.e.*, $\Delta m \ll M$) at different locations (x_c). The resonant frequency of the MSP with the mass load at different locations was determined using the numerical simulation with the properties and dimension listed in Table 1. Based on the resonant frequency, the S_m

of the MSP with the concentrated mass load at x_c is obtained, which is plotted in Figure 1. From the data shown in Figure 1, one can find that the S_m is symmetric about $x_c/L = 0.5$ as expected. Additionally, the S_m reaches the minimum value (*i.e.*, $S_m = 0$) at $x_c/L = 0.5$ and the maximum value ($S_{m,max}$) at two ends (*i.e.*, $x_c/L = 0$ and $x_c/L = 1$) which are consistent with the expectations and the experimental results [8].

3. Results and Discussion

The location dependence of the mass sensitivity for the MSPs with a concentrated mass has been experimentally characterized [8]. The experimental results show that the change in the resonant frequency due to the attachment of a concentrated mass is dependent on both the location and the resonant mode [8]. Based on the results reported in [8], one can conclude that: (1) the S_m for a concentrated mass at the node point (*i.e.*, $\varphi(x) = 0$) is zero; (2) the S_m reaches its maximum for a concentrated mass at the points at where the absolute value of the mode shape function, $|\varphi(x)|$, reaches its maximum; and (3) the S_m for a concentrated mass at a location (x) monotonically increases with the $|\varphi(x)|$. That is, the S_m has a tight relationship with the mode shape function. The physics behind this may be related to the influence of the mass load on the vibration behavior. When a mass load is attached to a resonator, there is a dragging force from the mass load to the resonator. The dragging force would be dependent on the acceleration of the mass load. For a resonator at one frequency with a concentrated mass at a location (x_c), the bigger the $|\varphi(x_c)|$ is, the higher the acceleration is. The higher the acceleration is, the stronger the influence on the resonant behavior is. Therefore, one can expect that the S_m for a concentrated mass at a location (x_c) monotonically increases with the $|\varphi(x_c)|$.

Based on these conclusions, an intuition take is that the $S_m(x)$ is proportional to $|\varphi(x)|^\alpha$ ($\alpha > 0$). If α is not an integer, the slope of the S_m at the node point is not continuous. When α is an integer, the slope of the S_m at the node point is not continuous if α (= 1, 3, 5, …) is odd number, but it is continuous if α (= 2, 4, 6, …) is an even number.

From the results shown in Figure 1, it is obtained that at two ends the S_m reaches its maximum, $S_{m,max}$, which is consistent with both the experimental results reported in [8] and the conclusion above since at two ends the $|\varphi(x)|$ reaches the maximum. Here, $S_{m,max} = 93.96$ Hz/ng, which is exactly the double of what S_m^{uni} obtained using Equation (1). Interestingly, it is also found that the simulated S_m *versus* x_c curve shown in Figure 1 can be well fitted with:

$$S_m(x_c) = \frac{S_{m,max}}{2}\left[1 + \cos\left(2\pi\frac{x_c}{L}\right)\right] = S_{m,max}\cos^2\left(\pi\frac{x_c}{L}\right) \tag{5}$$

It is well known that the mode shape function, $\varphi(x)$, for the fundamental resonant mode of an MSP without mass load can be written as [8]:

$$\varphi(x) = \cos(\pi\frac{x}{L}) \tag{6}$$

Based on the similarity between Equations (5) and (6), it is proposed that the S_m of an AW device to a concentrated mass at x_c can be determined by the corresponding mode shape function, $\varphi(x)$, as:

$$S_m(x_c) = C\varphi^2(x_c)\ (\Delta m << M) \tag{7}$$

where, C is a constant. The proposed Equation (7) is consistent with the intuition take from the experimental results reported in [8].

Considering a uniform mass load can be treated as a layer of concentrated mass, one should get:

$$S_m^{uni} = \int_0^L S_m(x)dx \qquad (8)$$

Combining Equations (7) and (8), the value of the constant "*C*" can be determined using the S_m^{uni}. Therefore, for an MSP with a concentrated mass at x_c, the S_m can be written as:

$$S_m(x_c) = 2S_m^{uni}cos^2\left(\pi\frac{x_c}{L}\right) \qquad (9)$$

From Equation (9), one can find that $S_{m,max} = 2S_m^{uni}$ for an MSP.

Based on above results, it is further introduced that Equations (7) and (8) can be used as a general methodology to determine the S_m of any AW device with a concentrated mass. In other words, the S_m of an AW device with a concentrated mass can be simply determined using the corresponding mode shape function, φ, for the AW device without mass load. To illustrate that this methodology can be used for all types of AW devices, two other types of AW devices (*i.e.*, cantilever and diaphragm) are studied here.

The cantilever has been widely studied as a high performance sensor platform in last two decades [6,9,10,21–23]. Various cantilevers, ranging in size from nanometers to micrometers, to even millimeters have been developed. For a one-end-fixed cantilever (length—*L*, width—*W*, thickness—*H*), the fundamental resonant frequency (f_0) of the cantilever without mass load is:

$$f_0 = \frac{\lambda_0^2}{4\pi}\frac{H}{L^2}\sqrt{\frac{E}{3\rho(1-\sigma^2)}} \; (L \gg W \gg H) \qquad (10)$$

where λ_0 (= 1.87510) is the dimensionless eigenvalue [6]. The mode shape function of this resonant mode is [22]:

$$\phi(x) = \cosh\frac{\lambda_0 x}{L} - \cos\frac{\lambda_0 x}{L} - \gamma_0\left(\sinh\frac{\lambda_0 x}{L} - \sin\frac{\lambda_0 x}{L}\right) \qquad (11)$$

where $\gamma_0 = \dfrac{\sinh\lambda_0 - \sin\lambda_0}{\cosh\lambda_0 + \cos\lambda_0}$, and the *x*-axis is defined as being along the length direction of the cantilever with $x = 0$ at the fixed end.

The S_m^{uni} of a cantilever can be calculated using Equations (1) and (10). However, the S_m of a cantilever with a concentrated mass is unknown. Due to the importance of the cantilever for the development of high-performance sensors, an effective-mass approach was used to determine the S_m of a cantilever with a concentrated mass at the free end (*i.e.*, $x = L$) [24]. It should be mentioned that the S_m for a cantilever with a concentrated mass at other locations cannot be determined even using this effective-mass approach. Based on this effective-mass approach with some approximations, it was concluded that the S_m of a cantilever with a concentrated mass at the free end is [24]:

$$S_m(L) \cong \frac{f_0}{2*0.24267*M} \text{ or } {S_m(L)}\Big/{S_m^{uni}} \cong 4.12 \qquad (12)$$

Using the methodology introduced here (*i.e.*, Equations (7) and (8)), the S_m of a cantilever with a concentrated mass at x_c can be easily written as:

$$S_m(x_c) = \frac{S_m^{uni}}{\int_0^L \varphi^2(x)dx}\varphi^2(x_c) \qquad (13)$$

where $\varphi(x)$ is given by Equation (11) and S_m^{uni} is determined by Equations (1) and (10). The location dependence of the S_m for a cantilever with a concentrated mass described by Equation (13) is shown in Figure 2. Based on Equation (13), the highest S_m is obtained for a cantilever with a concentrated mass load at the free end ($x = L$). That is, $S_{m,max} = S_m(L)$. This results in $\frac{S_m(L)}{S_m^{uni}} = 4.0$, which is very close to the result (~4.12) obtained from the effective-mass approach described above. Considering the approximations used in the effective-mass approach, one may conclude that the methodology introduced here is correct and good enough to determine the S_m of a cantilever with a concentrated mass at different locations.
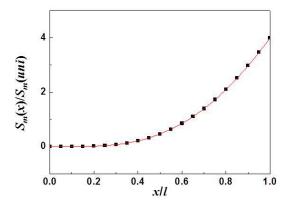

Figure 2. Mass sensitivity (S_m) of a cantilever with a concentrated mass *versus* the location (x) of the mass, where S_m is calculated using the methodology introduced here. The *y*-axis is normalized as $S_m(x)/S_m^{uni}$, where S_m^{uni} is defined by Equations (1) and (10).

Both MSPs and cantilevers studied above are one-dimensional devices. To further study the methodology introduced here, another AW device—two-dimensional diaphragm that has been used in the development of biological sensors [7,25]—is studied. A diaphragm can be either square or circular [7,26]. For a diaphragm with a square shape and a side length of "*a*" and a thickness of "*H*", the fundamental resonant frequency (f_0) is:

$$f_0 = \frac{\lambda_0^2}{4\pi} \frac{H}{a^2} \sqrt{\frac{E}{3\rho(1-\sigma^2)}} \, (a \gg H)$$

(14)

where $\lambda_0^2 = 35.99$ [27]. Therefore, the S_m^{uni} of a diaphragm can be calculated using Equations (1) and (14). The mode shape function of the fundamental resonant mode is [27]:

$$\phi(x, y) = \sin\frac{\pi x}{a} * \sin\frac{\pi y}{a}$$

(15)

where x and y are along two directions: length ($0 \leq x \leq a$) and width ($0 \leq y \leq a$).

Using the methodology introduced here (*i.e.*, Equations (7) and (8)), the S_m of a diaphragm with a concentrated mass at point (x_c, y_c) can be easily written as:

$$S_m(x_c, y_c) = \frac{S_m^{uni}}{\iint_0^a \varphi^2(x,y)dx \, dy} \varphi^2(x_c, y_c)$$

(16)

Based on Equation (16), one can obtain that the S_m reaches the maximum ($S_{m,max}$) at the center: $x_c = a/2$ and $y_c = a/2$, which is consistent with experimental results. From Equation (16), it is also obtained that $\frac{S_{m,max}}{S_m^{uni}} = 4.0$.

It should be mentioned that the S_m of a diaphragm with a concentrated mass at the center was determined using the effective-mass approach. The results of the effective mass approach show that the S_m of a diaphragm with a concentrated mass at the center is four times that for the diaphragm with a uniform mass load [25]. That is, for the concentrated mass at the center of a diaphragm, the conclusion of the effective-mass approach on the S_m is the same as that of the new methodology introduced here. This again confirms the correctness of the new methodology introduced here.

Application Remark: The methodology introduced here is used to determine the S_m for an ideally concentrated mass (*i.e.*, the volume is zero). In reality, a mass load is usually not an ideally concentrated mass, but is distributed over an area. If the area of a mass load is much smaller than the surface of the AW device, the methodology introduced here can be used as an approximation. If the area of a mass load is comparable with the surface of the AW device, the influence of the mass-load distribution has to be considered. In such case, one can treat a mass load over an area as an ideal mass load with a uniform distribution over the area. Therefore, the real mass sensitivity can be written as the integral of the S_m over the area. For example, if a mass load fully covers a segment of an MSP or a cantilever from $x = x_1$ to $x = x_2$, the real mass sensitivity ($S_{m,real}$) for this mass load should be:

$$S_{m,real} = \frac{S_m^{uni}}{\int_0^L \varphi^2(x)dx} \int_{x_1}^{x_2} \varphi^2(x)dx \qquad (17)$$

If the area of a mass load is smaller than the width of an MSP or a cantilever, the case cannot be treated as a one-dimensional case. However, an approximation approach can be used. For example, if a mass load covers an area of an MSP or a cantilever: along the length direction is from $x = x_1$ to $x = x_2$, along the width direction is wt% of the MSP/cantilever's width, the real mass sensitivity ($S_{m,real}$) for this mass load can be calculated approximately by:

$$S_{m,real} = (wt\%) \frac{S_m^{uni}}{\int_0^L \varphi^2(x)dx} \int_{x1}^{x2} \varphi^2(x)dx \qquad (18)$$

For a diagraph (*i.e.*, a two-dimensional case), the similar principle mentioned here can be used to calculate the sensitivity for a real mass load at different areas.

4. Conclusions

In conclusion, a numerical simulation approach was used to determine the influence of the mass-load location on the resonant frequency of the MSPs, which is used to determine the S_m for the MSPs with a concentrated mass at different locations. Based on the results, it is introduced that the S_m of an MSP with a concentrated mass can be simply determined using the mode shape function of the MSP without mass load. This methodology is further introduced as a general methodology to determine the S_m of any AW device. That is, the S_m of an AW device with a concentrated mass is proportional to the square of its mode shape function. This methodology was further proved using two widely used AW devices: (1) a one-dimensional cantilever; and (2) a two-dimensional diaphragm. Therefore, the S_m for any AW device with a concentrated mass can be simply determined using the mode shape function of the AW device without mass load.

Acknowledgments

Author Contributions

Zhang and Chai preformed the numerical simulation. Zhang prepared the figures. Zhang selected the MSP as the objective and corresponding materials properties. Cheng pioneered the concept for the methodology introduced here. Cheng and Zhang prepared the manuscript.

Conflicts of Interest

The authors declare no conflict of interest.

References

1. Ballantine, D.S.; White, R.M.; Martin, S.J.; Ricco, A.J.; Frye, G.C.; Zellers, E.T.; Wohltjen, H. *Acoustic Wave Sensors: Theory, Design and Physico-Chemical Applications*; Academic Press: New York, NY, USA, 1997.
2. Drafts, B. Coustic wave technology sensors. *IEEE Trans. Microw. Thery Tech.* **2001**, *49*, 795–802.
3. Ferreira, G.N.M.; da-Silva, A.C.; Tomé, B. Acoustic wave biosensors: Physical models and biological applications of quartz crystal microbalance. *Trends Biotechnol.* **2009**, *27*, 680–697.
4. Länge, K.; Rapp, B.E.; Rapp, M. Surface acoustic wave biosensors: A review. *Anal. Bioanal. Chem.* **2008**, *391*, 1509–1519.
5. Bănică, F.G. *Chemical Sensors and Biosensors: Fundamentals and Applications*; John Wiley & Sons: Chichester, UK, 2012.
6. Li, S.Q.; Orona, L.; Li, Z.; Cheng, Z.-Y. Biosensor based on magnetostrictive microcantilevers as a sensor platform. *Appl. Phys. Lett.* **2006**, *88*, doi:10.1063/1.2174092.
7. Yang, X.; Li, Z.M.; Odum, L.; Cheng, Z.-Y. Piezoelectric diaphragm as a high performance biosensor platform. *Appl. Phys. Lett.* **2006**, *89*, doi:10.1063/1.2396919.
8. Li, S.Q.; Cheng, Z.-Y. Non-uniform mass detection using magnetostrictive biosensors operating under multiple harmonic resonance modes. *J. Appl. Phys.* **2010**, *107*, doi:10.1063/1.3431523.
9. Ilic, B.; Czaplewsli, D.; Craighead, H.G.; Neuzil, P.; Campagnolo, C.; Batt, C. Mechanical resonant immunospecific biological detector. *Appl. Phys. Lett.* **2000**, *77*, 450–452.
10. Burg, T.P.; Godin, M.; Knudsen, S.M.; Shen, W.; Carlson, G.; Foster, J.S.; Babcock, K.; Manalis, S.R. Weighing of biomolecules, single cells and single nanoparticles in fluid. *Nature* **2007**, *446*, 1066–1069.
11. Zhang, K.W.; Fu, L.L.; Zhang, L.; Cheng, Z.-Y.; Huang, T.S. Magnetostrictive particle based biosensors for in situ and real-time detection of pathogens in water. *Biotech. Bioeng.* **2014**, *111*, 2229–2238.

12. Shih, W.Y.; Li, X.P.; Gu, H.M.; Shih, W.H.; Aksay, I.A. Simultaneous liquid viscosity and density determination with piezoelectric unimorph cantilevers. *J. Appl. Phys.* **2001**, *89*, 1497–1505.

13. Zhang, K.W.; Zhang, L.; Fu, L.L.; Li, S.Q.; Chen, H.Q.; Cheng, Z.-Y. Magnetostrictive resonators as sensors and actuators. *Sens. Actuators A Phys.* **2013**, *200*, 2–10.

14. Cheng, Z.Y. Applications of smart materials in the development of high performance biosensors. In Proceedings of 2005 MRS Fall Meeting, Boston, MA, USA, 27 November–2 December 2005.

15. Horikawa, S.; Bedi, D.; Li, S.; Shen, W.; Huang, S.; Chen, I.; Chai, Y.; Auad, M.L.; Bozack, M.J.; Barbaree, J.M.; *et al.* Effects of surface functionalization on the surface phage coverage and the subsequent performance of phage-immobilized magnetoelastic biosensors. *Biosens. Bioelectron.* **2011**, *26*, 2361–2367.

16. Chai, Y.T.; Wikle, H.C.; Wang, Z.Y.; Horikawa, S.; Best, S.; Cheng, Z.-Y.; Dyer, D.F.; Chin, B.A. Design of a surface-scanning coil detector for direct bacteria detection on food surfaces using a magnetoelastic biosensor. *J. Appl. Phys.* **2013**, *114*, doi:10.1063/1.4821025.

17. Li, S.Q.; Li, Y.G.; Chen, H.Q.; Horikawa, S.; Shen, W.; Simonian, A.; Chin, B.A. Direct detection of Salmonella typhimurium on fresh produce using phage-based magnetoelastic biosensors. *Biosens. Bioelectron.* **2010**, *26*, 1313–1319.

18. Liang, C.; Morshed, S.; Prorok, B.C. Correction for longitudinal mode vibration in thin slender beams. *Appl. Phys. Lett.* **2007**, *90*, doi:10.1063/1.2745262.

19. Zhang, K.W.; Zhang, K.H.; Chai, Y.S. Study of "blind point" and mass sensitivity of a magnetostrictive biosensor with asymmetric mass loading. *AIP Advances* **2014**, *4*, doi:10.1063/1.4878575.

20. Metglas information. Available online: www.metglas.com (accessed on 22 September 2015).

21. Johnson, B.N.; Mutharasan, R. Biosensing using dynamic-mode cantilever sensors: A review. *Biosens. Bioelectron.* **2012**, *32*, 1–18.

22. Ziegler, C. Cantilever-based biosensors. *Anal. Bioanal. Chem.* **2004**, *379*, 946–959.

23. Fu, L.L.; Zhang, K.W.; Li, S.Q.; Wang, Y.H.; Huang, T.-S.; Zhang, A.X.; Cheng, Z.-Y. *In situ* real-time detection of E. coli in water using antibody-coated magnetostrictive microcantilever. *Sens. Actuators B Chem.* **2010**, *150*, 220–225.

24. Yi, J.W.; Shih, W.Y.; Shih, W.H. Effect of length, width, and mode on the mass detection sensitivity of piezoelectric unimorph cantilevers. *J. Appl. Phys.* **2002**, *91*, 1680–1686.

25. Lu, X.; Guo, Q.S.; Xu, Z.; Ren, W.; Cheng, Z.-Y. Biosensor platform based on stress-imporved piezoelectric membrane. *Sens. Actuators A Phys.* **2012**, *179*, 32–38.

26. Lu, X.; Li, S.K.; Xu, Z.; Ren, W.; Cheng, Z.-Y. Piezoelectric member based biosensor platform. *Ferroelectrics* **2010**, *409*, 78–84.

27. Blevins, R.D. *Formula for Natural Frequency and Mode Shape*; Krieger Publising: New York, NY, USA, 1979.